Theor Chem Acc (2012) 131:1089
DOI 10.1007/s00214-012-1089-y

REGULAR ARTICLE

# Structure-stability diagrams and stability-reactivity landscapes: a conceptual DFT study

**Pratim Kumar Chattaraj · Ranjita Das · Soma Duley · Jean-Louis Vigneresse**

Received: 7 March 2011 / Accepted: 11 July 2011 / Published online: 4 February 2012


**Abstract** Electrophilicity and hardness have been shown to be adequate in constructing structure-stability diagrams. Maximum hardness principle and minimum electrophilicity principle provide a rough guide toward locating the domains of stability and reactivity in a fitness landscape. Bonding in solids, aromaticity, magic alkali clusters, bond—stretch isomers, multivalent superatoms, etc. have been analyzed within this purview.

**Keywords** Electrophilicity · Hardness · Structure · Stability · Reactivity

## 1 Introduction

Conceptual density functional theory [1–3] has been quite successful in providing quantitative definitions of popular qualitative chemical concepts like electronegativity ($\chi$) [4–6], hardness ($\eta$) [7, 8], and electrophilicity ($\omega$) [9–13]. It has also been shown to be adequate in obtaining theoretical justification of the associated electronic structure principles like the electronegativity equalization principle (EEP) [14–16], maximum hardness principle (MHP) [17–22], hard–soft acid–base principle (HSABP) [23–29], minimum electrophilicity principle (MEP) [30, 31], etc.

Attempts have been made [32] to propose simple structural coordinates to identify and to analyze the stable crystal structures of various solids. Different orbital radii [5, 33, 34], average principle quantum number [35], electronegativity difference [35, 36], hardness sum [36], etc. have been used as coordinates of the related structure-stability diagrams. In the present work, a new set of coordinates in terms of the hardness and the electrophilicity has been provided. An attempt has been made to provide a rationale through the connection between the electronic structure and the geometrical structure encompassing atoms, molecules, and solids. Different electronic structure principles may be used in analyzing the associated reactivity and stability.

Theoretical background of the current work has been presented in Sect. 2. Section 3 provides the computational details, and the results have been discussed in Sect. 4. Finally, Sect. 5 contains some concluding remarks.

## 2 Theoretical background

Global reactivity descriptors like electronegativity [4–6] and hardness [7, 8] are used to describe the reactivity of a molecule as a whole. For an $N$-electron system with total energy $E$, they are defined [4–8] as the following energy derivatives, within a conceptual density functional theory framework:

$$\chi = -\mu = -\left(\frac{\partial E}{\partial N}\right)_{v(\mathbf{r})} \tag{1}$$

and

$$\eta = \left(\frac{\partial^2 E}{\partial N^2}\right)_{v(\mathbf{r})} \tag{2}$$

Dedicated to Professor Eluvathingal Jemmis and published as part of the special collection of articles celebrating his 60th birthday.

P. K. Chattaraj (✉) · R. Das · S. Duley
Department of Chemistry and Center for Theoretical Studies, Indian Institute of Technology Kharagpur, Kharagpur 721302, India
e-mail: pkc@chem.iitkgp.ernet.in

J.-L. Vigneresse
Nancy-Université, UMR 7566 G2R, BP 23, 54501 Vandoeuvre cédex, France

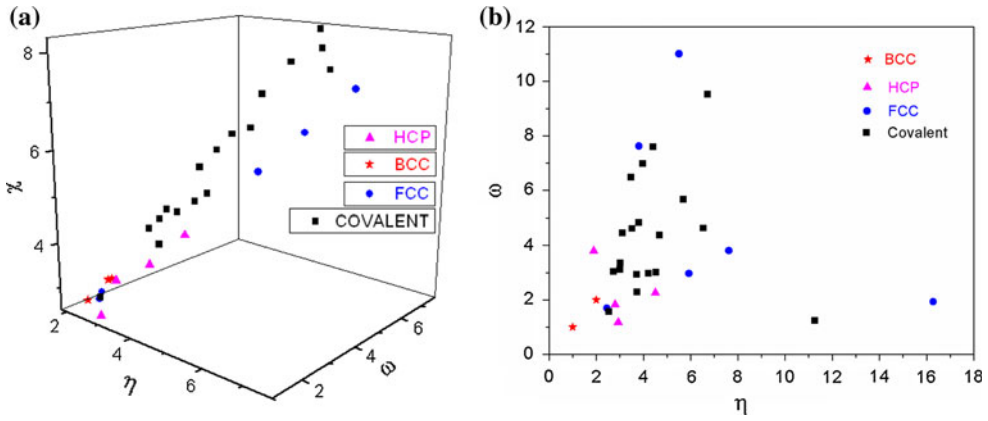


**Fig. 1** **a** 3-dimensional ($\chi$, $\eta$, and $\omega$) and **b** 2-dimensional ($\omega$ and $\eta$) plots of the crystal structure of the non-transitional elements

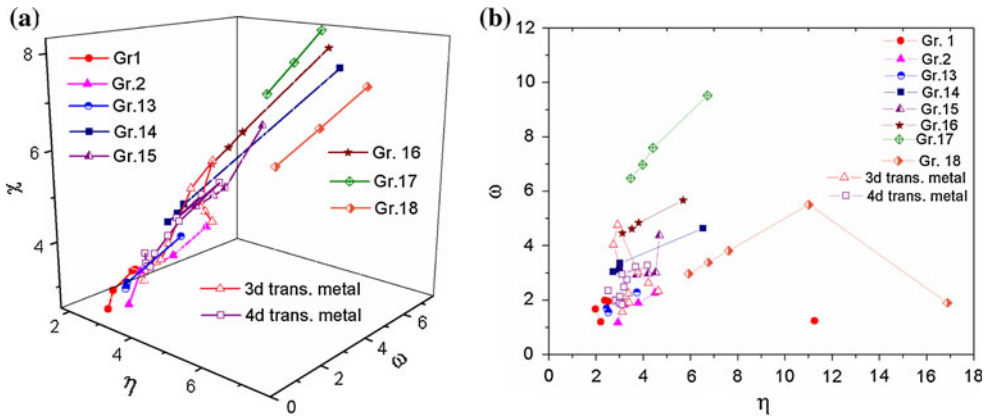


**Fig. 2** **a** 3-dimensional ($\chi$, $\eta$, and $\omega$) and **b** 2-dimensional ($\omega$ and $\eta$) plots of the elements up to $z = 54$

In the above equations, $\mu$ and $\upsilon(\mathbf{r})$ represent the chemical and external potentials, respectively.

Parr et al. [9] have defined an electrophilicity index ($\omega$) as follows:

$$\omega = \frac{\mu^2}{2\eta} = \frac{\chi^2}{2\eta} \tag{3}$$

For a stable state of a system or a favorable direction of a physico-chemical process, hardness often gets maximized [17–22] and electrophilicity gets minimized [30, 31]. While the maximum hardness principle (MHP) [17–22] is strictly valid [14–16] under the conditions of constant chemical and external potentials [17–22], validity of the minimum electrophilicity principle (MEP) [30, 31] requires that both hardness and electronegativity should attain their maximum values [31].

As hardness and electrophilicity are two important cardinal indices of stability vis-a-vis the two electronic structure principles stated above, it becomes quite legitimate to consider $\omega$ and $\eta$ as coordinates in the structure-stability diagrams complementing the previous studies [36] along these lines especially in connection with the nature of bonding in solids. The main aim of this paper is not to generate numbers but to analyze qualitative trends. The present study, in comparison to [36], increases the domain

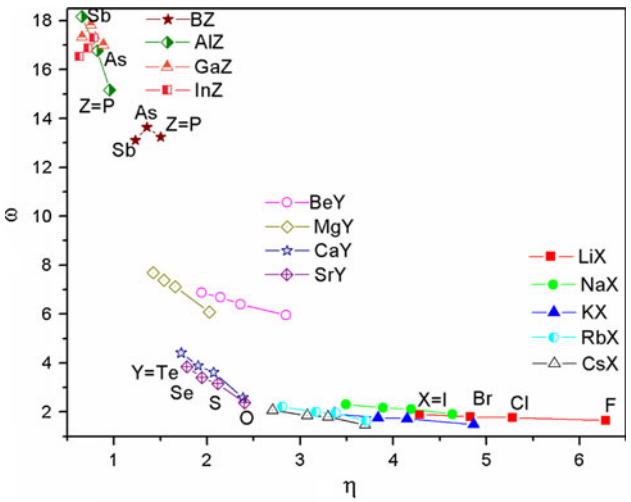


**Fig. 3** $\omega$ versus $\eta$ plot of binary octet compounds showing periodic trends

of applicability encompassing the stability of atoms, molecules, isomers, superatoms, clusters, and solids presumably by strengthening the rationale through the use of two well-accepted electronic structure principles, viz., the principles of maximum hardness and minimum electrophilicity within a broad conceptual DFT framework.

**Table 1** Crystal structure, electronegativity ($\chi$, eV), hardness ($\eta$, eV), and electrophilicity ($\omega$, eV) of binary octet compounds

| Compound | Crystal structures | $\chi$ | $\eta$ | $\omega$ | Compound | Crystal structures | $\chi$ | $\eta$ | $\omega$ |
|---|---|---|---|---|---|---|---|---|---|
| LiF | Rock Salt | 4.557 | 6.282 | 1.653 | SrS | Rock Salt | 3.652 | 2.116 | 3.152 |
| LiCl | Rock Salt | 4.323 | 5.280 | 1.770 | SrSe | Rock Salt | 3.636 | 1.943 | 3.403 |
| LiBr | Rock Salt | 4.175 | 4.827 | 1.805 | SrTe | Rock Salt | 3.703 | 1.783 | 3.846 |
| LiI | Rock Salt | 4.037 | 4.283 | 1.903 | ZnO | Wurtzite | 5.799 | 2.358 | 7.130 |
| NaF | Rock Salt | 4.210 | 4.633 | 1.912 | ZnS | Zinc Blende | 5.434 | 1.808 | 8.163 |
| NaCl | Rock Salt | 4.211 | 4.191 | 2.116 | ZnSe | Zinc Blende | 5.279 | 1.637 | 8.510 |
| NaBr | Rock Salt | 4.105 | 3.892 | 2.165 | ZnTe | Zinc Blende | 5.115 | 1.483 | 8.820 |
| NaI | Rock Salt | 4.011 | 3.495 | 2.302 | BN | Wurtzite | 7.598 | 1.921 | 15.021 |
| KF | Rock Salt | 3.809 | 4.863 | 1.491 | BP | Zinc Blende | 6.312 | 1.505 | 13.238 |
| KCl | Rock Salt | 3.783 | 4.149 | 1.725 | BAs | Zinc Blende | 6.083 | 1.356 | 13.646 |
| KBr | Rock Salt | 3.679 | 3.836 | 1.764 | BSb | Zinc Blende | 5.686 | 1.233 | 13.110 |
| KI | Rock Salt | 3.608 | 3.371 | 1.931 | AlN | Wurtzite | 5.798 | 1.564 | 10.751 |
| CsF | CsCl | 3.305 | 3.697 | 1.477 | AlP | Zinc Blende | 5.385 | 0.955 | 15.176 |
| CsCl | CsCl | 3.447 | 3.299 | 1.800 | AlAs | Zinc Blende | 5.254 | 0.823 | 16.778 |
| CsBr | CsCl | 3.388 | 3.077 | 1.865 | AlAb | Zinc Blende | 4.885 | 0.657 | 18.164 |
| CsI | CsCl | 3.338 | 2.704 | 2.060 | GaN | Wurtzite | 5.959 | 1.511 | 11.752 |
| RbF | Rock Salt | 3.494 | 3.710 | 1.645 | GaP | Zinc Blende | 5.491 | 0.886 | 17.009 |
| RbCl | Rock Salt | 3.634 | 3.380 | 1.954 | GbAs | Zinc Blende | 5.180 | 0.753 | 17.817 |
| RbBr | Rock Salt | 3.568 | 3.169 | 2.009 | GaSb | Zinc Blende | 4.779 | 0.659 | 17.330 |
| RbI | Rock Salt | 3.521 | 2.807 | 2.208 | InN | Wurtzite | 5.463 | 1.431 | 10.425 |
| BeO | Wurtzite | 5.823 | 2.850 | 5.949 | InP | Zinc Blende | 5.223 | 0.789 | 17.298 |
| BeS | Zinc Blende | 5.497 | 2.359 | 6.405 | InAs | Zinc Blende | 4.957 | 0.728 | 16.867 |
| BeSe | Zinc Blende | 5.354 | 2.144 | 6.686 | InSb | Zinc Blende | 4.571 | 0.632 | 16.522 |
| BeTe | Zinc Blende | 5.170 | 1.943 | 6.877 | | | | | |
| MgO | Rock Salt | 4.963 | 2.025 | 6.082 | | | | | |
| MgS | Rock Salt | 4.856 | 1.656 | 7.119 | | | | | |
| MgSe | Rock Salt | 4.760 | 1.536 | 7.378 | | | | | |
| MgTe | Rock Salt | 4.672 | 1.420 | 7.684 | | | | | |
| CaO | Rock Salt | 3.515 | 2.386 | 2.590 | | | | | |
| CaS | Rock Salt | 3.867 | 2.073 | 3.606 | | | | | |
| CaSe | Rock Salt | 3.849 | 1.905 | 3.888 | | | | | |
| CaTe | Rock Salt | 3.899 | 1.723 | 4.411 | | | | | |
| SrO | Rock Salt | 3.377 | 2.404 | 2.372 | | | | | |

Moreover, it provides comparable or better results than in [36], in all cases.

## 3 Computational details

In the present study, we analyze the periodic behavior of various atomic systems through the reactivity descriptors. We have taken the calculated values of $\chi$ and $\eta$ from Goycoolea et al. [37] except for H, He and Rb as was done before [38], since H and He are not available in Ref. [37] and presumably the corresponding values of Rb were in error. In the case of Rb, we have taken the calculated values of these two parameters from Robles and Bartolotti [39]. Geometry optimization and the frequency calculations of all the monocyclic hydrocarbons are performed at the B3LYP/6-311+G(d) level of theory by using the Gaussian 03 program [40], and for all the cases, the number of imaginary frequency turns out to be zero which confirms that they correspond to the minima on the potential energy surface (PES). In case of the molecules containing heavy atoms, the geometry optimization as well as frequency calculations are carried out at the B3LYP/6-311+G(d) level of theory for light atoms, whereas B3LYP/SDD level of theory is used for the heavy atoms within the molecules.

We have calculated the ionization potential ($I$) and the electron affinity ($A$) with the help of Koopmans' theorem [41] in terms of the appropriate frontier orbital energies:

$$I = -\varepsilon_{\mathrm{HOMO}};\ A = -\varepsilon_{\mathrm{LUMO}} \tag{4}$$

where $\varepsilon_{HOMO}$ and $\varepsilon_{LUMO}$ are the energies of the highest occupied and lowest unoccupied molecular orbitals, respectively. The global reactivity parameters, electronegativity ($\chi$) and hardness ($\eta$), are then calculated by using the following expressions:

$$\chi = -\mu = -\left(\frac{\partial E}{\partial N}\right)_{v(\mathbf{r})} \approx \left(\frac{I+A}{2}\right) \approx -\left(\frac{\varepsilon_{HOMO}+\varepsilon_{LUMO}}{2}\right) \tag{5}$$

and

$$\eta = \left(\frac{\partial^2 E}{\partial N^2}\right)_{v(\mathbf{r})} = \left(\frac{\partial \mu}{\partial N}\right)_{v(\mathbf{r})} \approx I - A \approx (\varepsilon_{LUMO} - \varepsilon_{HOMO}) \tag{6}$$

The electrophilicity index ($\omega$) has been calculated with the help of Eq. 3 and the above two equations.

## 4 Results and discussion

Fitness landscapes are constructed for various systems using electrophilicity and hardness as coordinates.

### 4.1 Solids

#### *4.1.1 Bonding in solids and periodicity*

Figure 1a depicts a three-dimensional plot using three reactivity descriptors $\chi$, $\eta$, and $\omega$ as structural parameters for 34 non-transitional elements originally considered in references [34] and [36] (but for H, He, F, and Ne in order that other points are distinctly visible). Conceptual DFT was used in describing solids earlier [42–44]. The most stable metallic structures of these elements as body-centered cubic (bcc), face-centered cubic (fcc), hexagonal closed packed (hcp), and covalent [36] are separated into different domains. In Fig. 1b, the corresponding $\omega$ versus $\eta$ plot is shown.

Periodic behavior of these elements are clearly delineated in Fig. 2 (Fig. 2b shows $\omega$ vs. $\eta$ plot) in which elements up to $z = 54$ are included (but for H, He, F, and Ne in order that other points are distinctly visible).

We plot in Fig. 3 $\omega$ versus $\eta$ for 56 binary octet compounds ($A^N B^{8-N}$) formed from the cations belonging to group-A (Table 1) as was studied in references [34] and [36]. Different zones corresponding to 8–8 CsCl, 6–6 Rock Salt, 4–4 Wurtzite, and 4–4 Zinc Blende structures are discernible. Associated periodic trends are also clearly manifested (Fig. 4). Relative hardness and electrophilicity values for various groups are as expected from chemical intuition.

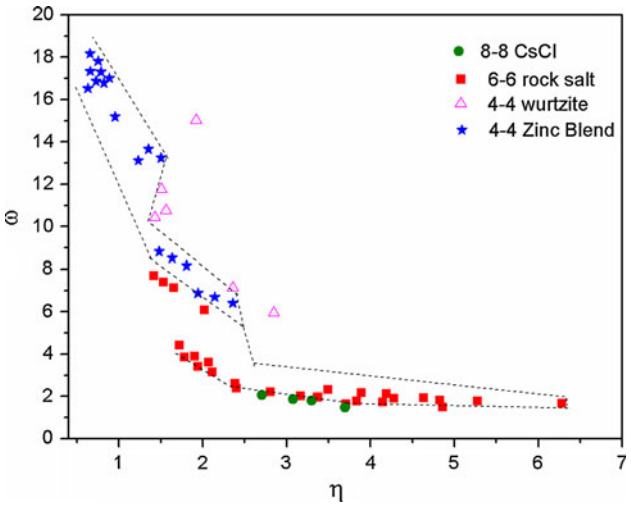


**Fig. 4** $\omega$ versus $\eta$ plot of binary octet compounds of group-A cations

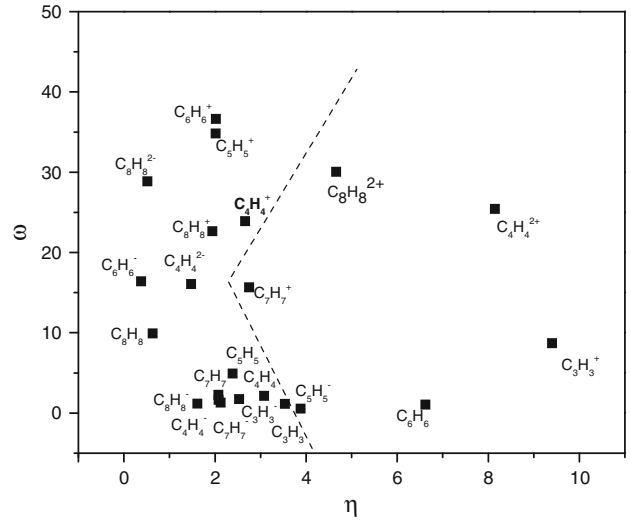


**Fig. 5** $\omega$ versus $\eta$ plot of monocyclic hydrocarbons

### 4.2 Atoms

#### *4.2.1 Stability and electronic structure principles*

Stability-reactivity landscapes may be generated by plotting electrophilicity versus hardness. A distinct stability pole would be the higher $\eta$-lower $\omega$ region and a reactivity pole would be lower $\eta$-higher $\omega$ region. Additional stability zones may be conceived via MHP [17–22] (only high $\eta$) or MEP [30, 31] (only low $\omega$). In Fig. 2, the noble gas elements appear in the most stable region, whereas halogens are shown to be highly reactive.

**Table 2** Energy ($E$, au), electronegativity ($\chi$, eV), hardness ($\eta$, eV), and electrophilicity ($\omega$, eV) of monocyclic hydrocarbons

| Hydrocarbon | E | $\chi$ | $\eta$ | $\omega$ |
|---|---|---|---|---|
| $C_3H_3$ | −115.97920 | 2.834 | 3.534 | 1.136 |
| $C_3H_3^-$ | −115.95603 | −2.970 | 2.530 | 1.743 |
| $C_3H_3^+$ | −115.75422 | 12.795 | 9.405 | 8.703 |
| $C_4H_4$ | −154.70362 | 3.643 | 3.077 | 2.156 |
| $C_4H_4^-$ | −154.71283 | −2.631 | 2.082 | 1.663 |
| $C_4H_4^+$ | −154.43119 | 11.281 | 2.661 | 23.911 |
| $C_4H_4^{2-}$ | −154.53046 | −6.893 | 1.478 | 16.077 |
| $C_4H_4^{2+}$ | −153.89256 | 20.352 | 8.144 | 25.430 |
| $C_5H_5$ | −193.50640 | 4.854 | 2.388 | 4.933 |
| $C_5H_5^-$ | −193.56993 | −2.093 | 3.880 | 0.565 |
| $C_5H_5^+$ | −193.18884 | 11.842 | 2.013 | 34.831 |
| $C_6H_6$ | −232.30073 | 3.743 | 6.617 | 1.058 |
| $C_6H_6^-$ | −232.24588 | −3.530 | 0.380 | 16.403 |
| $C_6H_6^+$ | −231.96608 | 12.166 | 2.020 | 36.626 |
| $C_7H_7$ | −270.94913 | 3.060 | 2.073 | 2.258 |
| $C_7H_7^-$ | −270.95602 | −2.359 | 2.123 | 1.311 |
| $C_7H_7^+$ | −270.60691 | 9.285 | 2.749 | 15.676 |
| $C_8H_8$ | −309.55802 | 3.535 | 0.629 | 9.928 |
| $C_8H_8^-$ | −309.56857 | −1.942 | 1.611 | 1.170 |
| $C_8H_8^+$ | −309.33059 | 9.374 | 1.940 | 22.647 |
| $C_8H_8^{2-}$ | −309.42749 | −5.449 | 0.514 | 28.878 |
| $C_8H_8^{2+}$ | −308.91526 | 16.737 | 4.661 | 30.052 |

## 4.3 (Anti) aromatic molecules

### *4.3.1 Aromaticity*

Figure 5 presents the $\omega$ versus $\eta$ plot (Table 2) for some monocyclic hydrocarbons and their ions. Majority of the aromatic species [45] with $(4n + 2)$ $\pi$ electrons fall on the stability domain. Anions and dianions exhibit large $\omega$ values mainly because of the negative (large) $\chi$ values and the quadratic appearance of the latter in Eq. 3. It may be noted that these fitness landscapes provide only a rough guide toward the stability and reactivity and the associated electronic structure principles (MEP and MHP) provide an approximate rationale for the same.

## 4.4 Metal clusters

### *4.4.1 Magic alkali clusters*

It is known that the alkali metal clusters with a magic number of atoms are more stable in comparison to their neighbors [46–50]. We have taken the calculated $\eta$ and $\omega$ values for $Li_n$ and $Na_m$ clusters from Chattaraj et al. [50]. Figure 6 provides the $\omega - \eta$ landscapes of $Li_n$ (Fig. 6a) and $Na_m$ (Fig. 6b) clusters. As expected, the magic clusters occupy the most stable zone.

## 4.5 Isomers

### *4.5.1 Bond-stretch isomerism*

A family of $Be_6Zn_2^{2-}$ clusters exhibits bond-stretch isomerism [51]. Figure 7 presents the $\omega - \eta$ landscape of these clusters (shown at the bottom of the Fig. 7). While more stable clusters (according to their relative energy values) appear in the high $\eta$-low $\omega$ region, the three least stable isomers appear in the low $\eta$-high $\omega$ zone**.** Values of $\eta$ and $\omega$ were calculated using a $\Delta$SCF method in [51], whereas the present work makes use of Koopmans' theorem.

## 4.6 Superatoms

### *4.6.1 Multivalent superatoms*

Some atomic clusters exhibit the characteristics of a single atom in its elemental state [52]. Properties of a halogen atom are revealed by $Al_{13}$ and those of an alkaline earth metal atom is followed by $Al_{13}^+$. Behavior of a noble gas atom is

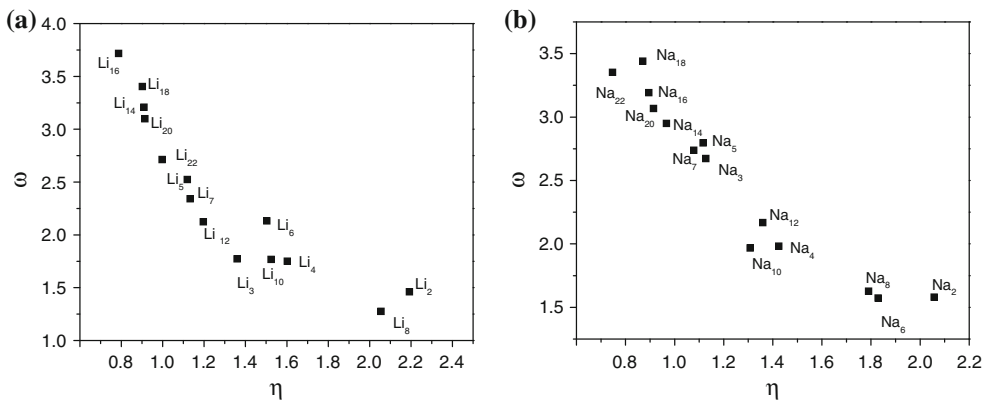


**Fig. 6** $\omega$ versus $\eta$ plots of **a** $Li_n$ and **b** $Na_m$ clusters

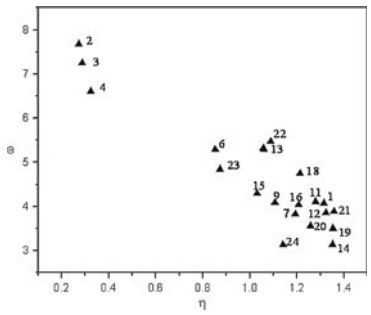


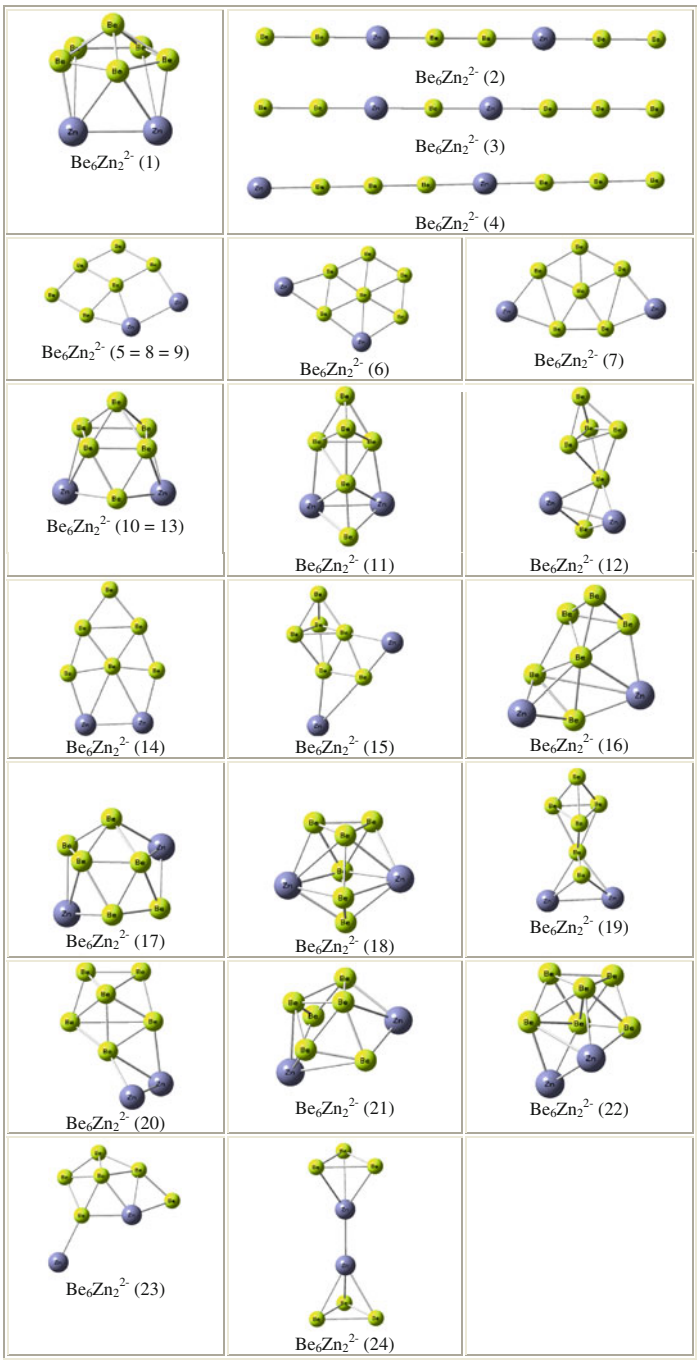


Reprinted with permission from ref 51. Copyright 2010 Taylor and Francis: Florida.

**Fig. 7** $\omega$ versus $\eta$ plot of different bond-stretch isomers of $Be_6Zn_2^{2-}$ clusters

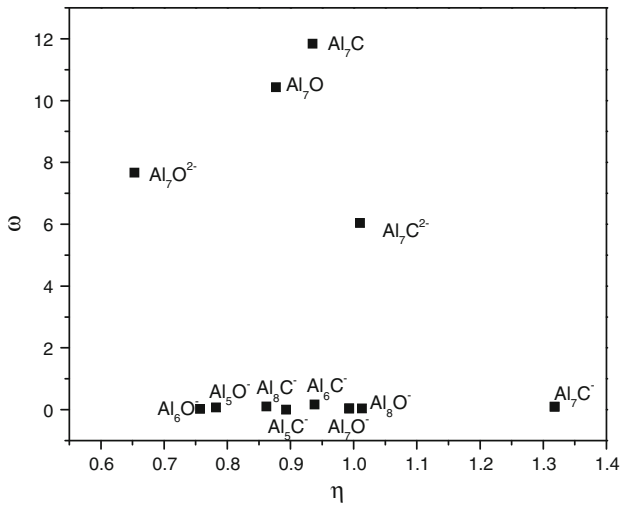


**Fig. 8** $\omega$ versus $\eta$ plots of different $Al_7M^{n-}$ (M = C, O) clusters and different $Al_mM^-$ (M = C, O) clusters ($m$ = 5–8; $n$ = 0, 2)

exhibited by a superatom $Al_{13}^-$. Multivalent superatoms like $Al_7C^-$ and $Al_7O^-$ are aromatic [53] and stable relative to their neighbors. Figure 8 depicts the $\omega - \eta$ landscape of these superatom ($Al_7C^-$ and $Al_7O^-$) and their neighbors formed by varying the number of Al atoms and the number of electrons. The $\eta$ and $\omega$ values are taken from Ref. [53]. The stable superatoms occupy the most stable zone. Based on the HOMO–LUMO gaps and the $\Delta\Delta E$ values $Al_7C^-$ is found to be the most stable cluster among these superatoms, which is faithfully mimicked by the stability-reactivity landscape.

## 5 Concluding remarks

Nature of bonding in different solids can be described by global reactivity descriptors like electrophilicity and hardness. Conceptual density functional theory based electronic structure principles such as the principles of maximum hardness and minimum electrophilicity may be utilized in understanding the stability associated with aromatic systems, magic clusters, bond-stretch isomers, and superatoms through identification of a stability zone in a fitness landscape.

**Acknowledgments** We are delighted to dedicate this paper to Professor E. D. Jemmis, a pioneer in the computational chemistry research in India, on his sixtieth birthday. PKC would like to thank Professor P. V. Bharatam, G. Frenking, and G. N. Sastry for kindly inviting him to contribute in this special issue of Theoretical Chemistry Accounts. PKC also thanks DST, New Delhi for the J. C. Bose Fellowship. RD and SD acknowledge the financial assistance from UGC, New Delhi, and CSIR, New Delhi, respectively.

## References

1. Parr RG, Yang W (1989) Density functional theory of atoms and molecules. Oxford University Press, Oxford
2. Geerlings P, De Proft F, Langenaeker W (2003) Chem Rev 103:1793
3. Chattaraj PK (ed) (2009) Chemical reactivity theory: a density functional view. Taylor and Francis/CRC Press, Florida
4. Mulliken RS (1934) J Chem Phys 2:782
5. Pauling L (1960) The nature of the chemical bond. Cornell University Press, Ithaca
6. Parr RG, Donnelly RA, Levy M, Palke WE (1978) J Chem Phys 68:3801
7. Parr RG, Pearson RG (1983) J Am Chem Soc 105:7512
8. Pearson RG (1997) Chemical hardness: applications from molecules to solids. Wiley-VCH, Weinheim
9. Parr RG, Szentpály Lv, Liu S (1999) J Am Chem Soc 121:1922
10. Chattaraj PK, Sarkar U, Roy DR (2006) Chem Rev 106:2065
11. Chattaraj PK, Roy DR (2007) Chem Rev 107:PR46
12. Chattaraj PK, Giri S (2009) Annu Rep Prog Chem Sect C 105:13
13. Chattaraj PK, Giri S, Duley S (2011) Chem Rev 111:PR43
14. Sanderson RT (1951) Science 114:670
15. Sanderson RT (1954) J Chem Educ 31:238
16. Sanderson RT (1955) Science 121:207
17. Pearson RG (1987) J Chem Educ 64:561
18. Pearson RG (1993) Acc Chem Res 26:250
19. Pearson RG (1999) J Chem Educ 76:267
20. Parr RG, Chattaraj PK (1991) J Am Chem Soc 113:1854
21. Chattaraj PK, Liu GH, Parr RG (1995) Chem Phys Lett 237:171
22. Ayers PW, Parr RG (2000) J Am Chem Soc 122:2010
23. Pearson RG (1973) Hard and soft acids and bases. Dowden, Hutchinson and Ross, Stroudsberg, PA, Hancock, RD
24. Pearson RG (1990) Coord Chem Rev 100:403
25. Chattaraj PK, Lee H, Parr RG (1991) J Am Chem Soc 113:1855
26. Chattaraj PK, Schleyer PvR (1994) J Am Chem Soc 116:1067
27. Martell AE (1996) J Chem Educ 73:654
28. Chattaraj PK, Gomez B, Chamorro E, Santos J, Fuentealba P (2001) J Phys Chem A 15:8815
29. Chattaraj PK, Maiti B (2003) J Am Chem Soc 125:2715
30. Chamorro E, Chattaraj PK, Fuentealba P (2003) J Phys Chem A 107:7068
31. Parthasarathi R, Elango M, Subramanian V, Chattaraj PK (2005) Theor Chem Acc 113:257
32. Philips JC (1977) Festkorper probleme XVII: advances in solid state physics. In: Trensch J (ed) Viewing, Braunschweig
33. Simon G, Bloch AN (1973) Phys Rev B 7:2754
34. St. John J, Bloch AN (1974) Phys Rev Lett 18:1095
35. Mooser E, Pearson WB (1959) Acta Crystallogr 12:1015
36. Sankar S, Parr RG (1985) Proc Natl Acad Sci USA 82:264
37. Goycoolea C, Barrera M, Zuloaga F (1989) Int J Quantum Chem 36:455
38. Chattaraj PK, Maiti B (2001) J Chem Edu 78:811
39. Robles J, Bartolotti LJ (1984) J Am Chem Soc 106:3723
40. Gaussian 03W, revision B.03 (2003) Gaussian, Inc., Pittsburgh
41. Koopmans TA (1933) Physica 1:104
42. Van Genechten KA, Mortier WJ, Geerlings P (1986) Chem Comm 646:1278
43. Van Genechten KA, Mortier WJ, Geerlings P (1987) J Chem Phys 86:5063
44. Uytterhoeven L, Mortier WJ, Geerlings P (1989) J Phys Chem Solids 50:479
45. Hückel E (1931) Z Phys 70:204
46. Harbola MK (1992) Proc Natl Acad Sci USA 89:1036
47. Solov'yov IA, Solov'yov AV, Greiner W (2002) Phys Rev A 65:053203
48. Chandrakumar KRS, Ghanty TK, Ghosh SK (2004) J Chem Phys 120:6487
49. Jose KV J, Gadre SR (2008) J Chem Phys 129:164314
50. Chattaraj PK, Duley S, Das R (2010) Chem Educator 15:474

51. Giri S, Abhijith Kumar RPS, Chakraborty A, Roy DR, Duley S, Parthasarathi R, Elango M, Vijayaraj R, Subramanian V, Merino G, Chattaraj PK (2010) Bonding, aromaticity and possible bond-stretch isomerism in an "All-Metal" cluster—$[Be_6Zn_2]^{2-}$. In: Chattaraj PK (ed) Aromaticity and metal clusters. Taylor and Francis, Florida
52. Reveles JU, Khanna SN, Roach PJ, Castleman AW Jr (2006) Proc Natl Sci Acad 103:18405
53. Chattaraj PK, Giri S (2007) J Phys Chem A 111:11116